An Accessible Virtual Reality Model of Surgical Microscopy for Microsurgical Practice

Haochen Wang[1*], Samuel S. Neuman[1*], Sahand C. Eftekari[2], Ellen C. Shaffrey[3], and Samuel O. Poore[3] ✉

[1]Department of Biomedical Engineering, Univeristy of Wisconsin-Madison, Madison, WI, USA
[2]School of Medicine and Public Health, Univeristy of Wisconsin-Madison, Madison, WI, USA
[3]Department of Surgery, Division of Plastic Surgery, University of Wisconsin-Madison, Madison, WI, USA
[*]H.W. and S.S.N contributed equally to this work.

Access to realistic training modules and equipment plays a large role in the global need for microsurgery procedures. Many surgeons surveyed around the globe report a lack of equipment and lack of training exposure as a barrier to incorporating microsurgical procedures in their practice, and many students experienced reduced training hours in the OR during the COVID-19 pandemic. In this study, we present a novel approach for microsurgical training and procedures utilizing multiple webcams to create a realistic stereoscopic view of the surgical specimen. Using a calibration and normalization algorithm, the images are streamed over a local server and displayed in the 3D virtual reality space with the capacity for digital zoom. Object-oriented programming was used to minimize computational demand and latency in streaming to create real-time images for the user. This design will undergo rigorous testing on the latency and clarity of the images. Quantification of image quality will be used to create accurate mapping of the images on the VR canvas. Medical trainees of various stages will be asked to provide numerical rating on various aspects of the design, and a linear regression will show how stage of training confers certain benefits and challenges with the use of this design relevant to replacement of commercial microscopes.

Microsurgery | Surgical Education | Virtual Reality
Correspondence: ***poore@surgery.wisc.edu***

Introduction

Microsurgery, or the performance of surgery under a microscope, has been an integral part of surgical residency curricula since the 1960s. Anastamosis, or the surgical joining of blood vessels, can be used to join vessels of 1mm diameter. Microsurgery is thus one of the most technically demanding surgical techniques; recommended training includes a 40 course on the basics of the technique, and three months of integration into a resident's practice is considered the minimum to achieve proficiency (1). Previous work has shown standardized eight-week courses in residency improve time-to-completion and latency in trials of anastamosis in animal models (2, 3).

Significant barriers to microsurgical practice exist for surgeons operating in communities with limited technical resources. A survey conducted in Latin American found that orthopedic surgeons in high-income countries were up to 45% more likely to perform free-flap sugeries than orthopedic surgeons in middle-income countries, and only 44% of orthopedic surgeons had received formal training in soft tissue surgery in all nations surveyed (4). A survey in African nations found that 84% of microsurgeons agreed that there is a current shortage of surgical expertise in their region, and 81% agreed that the lack of instruments and resources is a hindrance (5).

Cost-effective solutions to current global limitations in microsurgical training are urgently needed (6, 7). Popular surgical microscopes can exceed $100k USD; when this cost is distributed to the patient, the use of a microscope adds during surgery adds a minimum of $2k USD to the cost of the procedure (8). The costs associated with surgical microscope use are higher outside of the US and Europe (9). For the training microsurgeon, access to commercial microscopes is further limited by their portability, size, and durability (10). This became apparent during the COVID-19 pandemic when surgical residents had limited hands-on operative hours and were limited to virtual instructional modes (11, 12).

While numerous devices have been proposed to fill the need for an affordable model of the surgical microscope, no self-contained devices exist that can accurately mimic the experience of the microscope. Stereotactic vision is an ubiquitous feature of modern surgical microscopes (10) and allows the user to perceive three dimensions in their field of view in a manner similar to unassisted human vision. Cameras integrated into smartphones allow for digital zoom and livestreaming of the acquired image, and because of their popularity, smartphones are an attractive option for microscopic vision. Previous work involving the use of smartphones has been successful as an alternative to commercial microscopes; standardized trials of anastamoses performed by surgical residents using a suspended smartphone camera found no difference in operation times or ALI scores when compared to a commercial microscope (13). Virtual Reality provides users with an immersive three-dimensional field of view and can allow for the perception of stereotactic vision when the two eyes are presented different images. Previous work has found success in streaming images taken through the objectives of a commercial microscope to a VR headset (14), though this design encountered significant delays in the projection of the image to the user.

In this study, we propose a simple model for microsurgical practice that is comparable to commercial surgical microscopes while maintaining accessibility. Our design utilizes two Logitech webcams in an array with fixed horizontal disparity and angles of projections. The webcams are connected to a laptop computer via hardwire connection. Within Unity

software, basic manipulations are made to position the two images in 3D virtual space before the images are streamed through a local server to an Oculus VR headset. The user is able to visualize the surgical specimen on the field with optimal ergonomics through a stable local connection with minimal lag.

Results

The Proposed Design.

The proposed model of the surgical microscope achieves stereoscopic vision via the use of two webcams with disparate perspectives. The webcams are held in place by a 3D printed fixture such that their horizontal disparity and angle of projection are constant, 60mm and 9°, respectively (Fig. 1).

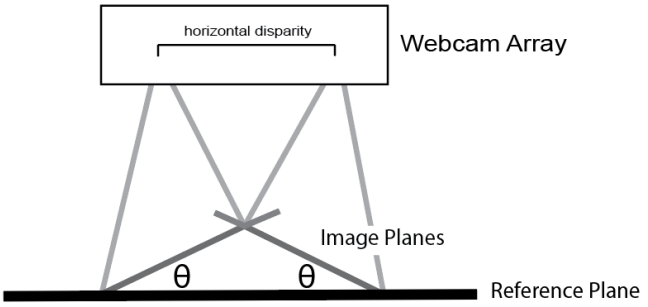

Fig. 1. The geometry of the webcam array. Two webcams are fixed within the 3D printed array such that they are located at a fixed horizontal disparity and angled downwards at an angle θ relative to the norm of the reference plane. Two respective image planes are acquired, each inclined at angle θ from the reference plane. The discrepancies in the two image planes allow for the perception of stereoscopic vision for the user.

The design can be divided into four aspects (Fig. 2). First, the initiated webcams acquire the two images needed for stereoscopic vision. The two images acquired by the webcams are then sent to the computer through a wired connection. The two webcam inputs are declared in Unity Software (v. 2020.3.14f1, San Francisco, CA) using $C\#$ Code. After declaration of the webcam inputs, the code allows Unity to toggle the image input source - in use, the user would set the input source to the two external webcams. This is done by pressing a button on the user interface. For each declaration of the input, the code allows for mapping of a second button on the user interface that serves as an on/off switch for the image input. This is achieved by a punctuated mechanism as the image build is turned off when a floating operator is set to null, and reassignment of the operator to a non-null value turns the camera on when selected by the user. The source code can be found in Supp. Note 1.

Modifications to the images are necessary for the perception of the field of view. First, in Unity, the left and right images are spliced and mapped to the 3D canvas vector space. Their exact position will be calibrated to match the distance between human pupils with no vertical offset. Because the size of the images are exported by the webcams with the minimum aspect ratio, linear transformations will be applied such that the size of the image is meaningful to the user. This capability of the design allows for 'digital zoom' of the images,

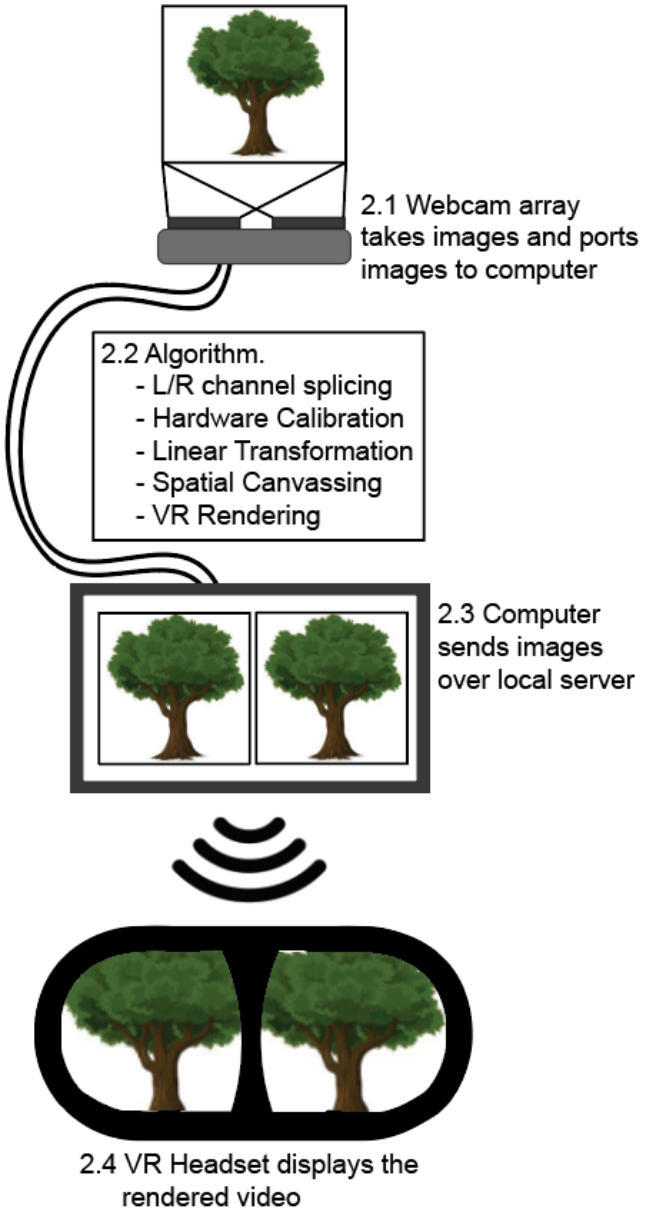

Fig. 2. Schematic of the VR Microsurgery Model. The transfer of information can be divided into four phases. First, the webcam array acquires the two offset images of the surgical specimen. The two images are sent to the laptop computer via hardwire connection. After this, the computer performs an algorithm to calibrate and render the images in 3D space. The computer then sends the images through a wireless connection to a local server to the Oculus VR headset. Finally, the user views the images on the 3D canvas.

or an artificial magnification of the images to resolve finer details of the specimen. The two images are then placed on the spatial canvas such that their position is always in front of the user and not fixed in space. The canvas is rendered in Unity software. Information on the rendered canvas is sent wirelessly through a local server to an Oculus Quest 2 VR Headset (Meta, Irvine, CA). The canvas is oriented on the canvas such that the broader visual context of the user can be seen in their peripheral vision.

Similar to a commercial surgical microscope, this device can achieve magnified stereoscopic vision with minimal and negligible latency due to wireless streaming. It is portable

Table 1. Itemized expenses associated with design construction

Item	Quantity	Unit Price ($USD)
Webcam	2	25
3D Printed Webcam Array	1	10
USB Cables	2	5
Oculus Headset	2	500
Total		570

and requires minimal setup, making it optimal for use by medical students, surgery residents, and physicians with limited access to commercial surgical microscopes. The device is affordable (Table 1) when compared to current commercial microscopes (10).

Discussion

Limitations and Consideration of the Current Design.

Because this design relies on fixed calibration parameters, any adjustments made to the focal distance, camera angles, or size of surgical specimen may create misalignment of the images in the 3D canvas. Further work is needed to account for changes in focal distance and focus of the webcams, and a temporary solution will be applied for testing that disables the autofocus of the cameras. Additionally, the design in its current iteration is prone to obsolescence due to the frequent package updates pushed by Unity. A stable source code library would need to be maintained for long-term use.

While this design represents great progress in an accessible model of a surgical microscope, it still relies on existing hardware and infrastructure. Our device relies on the ability of the surgeon to provide a laptop computer, Oculus headset, stable internet connection (Table 1), both of which are not guaranteed for plastic surgeons around the world (15). The advantages conferred by the integration of these devices include the ability to remotely stream surgeries, which may help increase exposure when in-person training is not possible (11, 12).

Data obtained from testing is intended to quantify image quality and latency as well as the useful of the device of inexperienced and experienced surgeons. Implicit in our comparison is the assumption that the skills acquired through training on commercial microscopes is translatable to our VR system. It is possible that these surgeons experience more difficulty while using this device; post hoc interpretations of this data will require their responses on the exit survey.

Progress in Unity Project Development.

The current version of Unity project uses WebSocket protocol to set up wireless communication between the sender device (computer) and the receiver device (Oculus Quest 2). However, compatibility issues arose in Unity with the current build after a major update, and the communication between Oculus and computer could not be restored after version rollback. Future efforts involve the utilization of packages such as "WebSocket-Sharp" (to enable WebSocket protocol to run in $C\#$) and other native Unity functions such as "Unity Render Streaming" (to utilize new streaming protocols for the project). The team will begin testing according to the protocols detailed in method section as soon as the communication is settled.

Methods

Calibration and Determination of Image Quality of the VR Training Model.

Image quality is defined as resolution and image deformation. To quantify image deformation, seven 1cm×1cm squares will be drawn on standard graph paper atop the surgical training station. The pixels nearest the each edge of the square will be measured with Fiji package of ImageJ developed by Schindelin *et al.* (16). Expected pixel size of the squares at 1080p resolution will be determined and compared with the true measurements. Image deformation due to streaming is defined as the percent change in the displayed lengths of each square, and the overall deformation will be reported as normalized vectors on the horizontal and vertical direction for both visual channels. An example of this calibration is given in Fig. 3, where X_L and Y_L represent the left and right horizontal offset, and Y represents the vertical offset between the two hemifields.

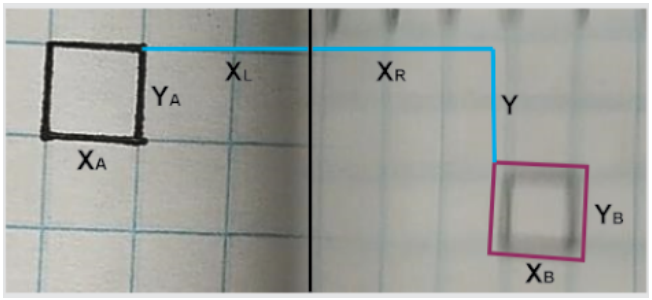

Fig. 3. Image analysis framework for calibration of horizontal and vertical displacements. Any discrepancies in the size of the boxes between the two hemispheres will be normalized by area (red square). The horizontal displacements X_L and X_R and vertical displacement Y will be measured using the line function in ImageJ.

Equations for the displacement of vertical and horizontal corrections are derived from trigonometric relationships regarding the natural angle of the webcams in their array with known focal distance F between the mirror array and surgical specimen.

$$\Delta\theta_y = F \times arcsin(Y) \quad \textbf{(1)}$$

$$\Delta\theta_x = F \times arcsin(X_L - X_R) \quad \textbf{(2)}$$

We define normalization matrices $\mathbf{A}$ and $\mathbf{B}$ such that:

$$\mathbf{A} = \begin{bmatrix} X_A & 0 \\ 0 & Y_A \end{bmatrix} \qquad \mathbf{B} = \begin{bmatrix} X_B & 0 \\ 0 & Y_B \end{bmatrix} \quad \textbf{(3)}$$

To prove they exist in the same vector space, we declare $\mathbf{S}$ with angle θ between the focal rays of the camera and the norm of the reference plane (Fig. 1) such that:

$$\text{define } S \in \mathbb{R} = \begin{bmatrix} cos(\theta) & 0 \\ 0 & 1 \end{bmatrix} \quad \textbf{(4)}$$

Then:

$$det(\mathbf{A}) = det(\mathbf{B} \times \mathbf{S}) = area = X_i Y_i cos(\theta) \quad \textbf{(5)}$$

Measurement of the Time Delay due to Wireless Streaming.

Time delay in streaming is defined as the time interval between the events of the user's operation and the display of the events on the VR headset. The VR training system will be set to record a stop watch displayed on a laptop screen. A smartphone will be used to record the displays of Oculus VR headset and the laptop screen simultaneously. Randomly choosing five timestamps in the recorded video, the difference in the time between the true and streamed images will be measured and reported as the average as time delay due to wireless streaming.

Evaluate Effectiveness of VR System in Microsurgery Training.

Participants will be recruited (n>20) with informed consent and asked to take a background survey on their current level of experience in microsurgical training. The participants will be divided into two groups based on level of experience for microsurgery training with microscopes. Medical students and residents will be divided by whether they self-identify as having "little to no prior microsurgery training experience" or "extensive microsurgery training experience". Participants in both groups will be randomly assigned to M-V or V-M groups, where the letter denotes the whether the microsurgery training sessions with involve the commercial microscope (M) or VR system (V). After a brief, standardized training session on their respective device, students will be requested to perform anastomosis procedures on samples of chicken breast. Each participant will perform two sets of three trials; the first set will be performed on larger blood vessels requiring 8 stitches, and the second set will be performed on smaller blood vessels requiring 5 stitches. After a rest of one hours, participants will perform the same sets of anastomosis procedures using the equipment they did not previously use. The time spent on the task will be recorded for each trial of microsurgery practice. Student's T-test will be used to find if there is is a statistical difference in the time to complete the procedures for familiar and unfamiliar groups.

Analysis of User Experience with the VR Training Model.

After anastomosis sessions, participants will invited to take a short exit survey regarding their experience with the VR training models. On a scale of 1-5, with 1 being most negative and 5 being most positive, participants will be asked to rate their user experiences based on factors such as "Ease of Use," "Learning Effort," and "How well the VR training model simulated experience with microscopes." Numerical ratings will analyzed using Student's T-test to investigate emerging trends underlying the user feedback. Using user background as features and their numerical ratings as labels, a least-square regression equation will be generated to predict if the VR training model would be acceptable for microsurgery trainees at different stages of training. The relationship between features ($\mathbf{X}$) and the labels ($\mathbf{Y}$) will be characterized via a weight matrix ($\mathbf{W}$):

$$\mathbf{XW} = \mathbf{Y} \quad \textbf{(6)}$$

Where the weight matrix can be derived as:

$$\mathbf{W} = (\mathbf{X}^T\mathbf{X})^{-1}\mathbf{X}^T\mathbf{Y} \quad \textbf{(7)}$$

Then, using test features ($\mathbf{X}'$), average of features for each group (such as medical trainees versus faculty staff, experienced users versus beginners), expected user rating on the VR training model ($\mathbf{Y}'$) can be determined as:

$$\mathbf{Y}' = \mathbf{X}'\mathbf{W} \quad \textbf{(8)}$$

ACKNOWLEDGEMENTS
We would like to thank Alexander Vazquez for his help in the conception of the design, Dr. Puccinelli for coordinating BME Design, and the UW Makerspace.

Bibliography

1. Vinagre, G., Villa, J. and Amillo, S. Microsurgery training: does it improve surgical skills? *Journal of Hand and Microsurgery*, 9:047–048, 2017.
2. Di Cataldo, A., Li Destri, G., Trombatore, G., Papillo, B., Racalbuto, A., and Puleo, S. Usefulness of microsurgery in the training of the general surgeon. *Microsurgery*, 18:446–448, 1998.
3. Ko, J.W., Lorzano, A., and Mirarchi, A.J. Effectiveness of a microvascular surgery training curriculum for orthopaedic surgery residents. *Journal of Bone and Joint Surgery*, 97:950–955, 2015.
4. MacKechnie, M.C., Flores, M.J., Giordano, V., Terry, M.J., Garuz, M., Lee, N., Rojas, L.G., MacKechnie, M.A., Bidolegui, F., Brown, K., and Quintero, J.E. Management of soft-tissue coverage of open tibia fractures in Latin America: Techniques, timing, and resources. *Injury*, 53:1422–1429, 2022.
5. Banda, C.H., Georgios, P., Narushima, M., Ishiura, R., Fujita, M., and Goran, J. A comparison of using a smartphone versus a surgical microscope for microsurgical anastomosis in a non-living model. *Journal of Plastic, Reconstructive, and Aesthetic Surgery*, 20:19–26, 2019.
6. Wilkinson, E., Aruparayil, N., Gnanaraj, N., Brown, J., and Jayne, D. Barriers to training in laparoscopic surgery in low- and middle-income countries: A systematic review. *Tropical Doctor*, 51:408–414, 2021.
7. Nguyen, H.N., Chen, J., Nguyen, T.V., Le, D.T., Nguyen, T.S., and Jeng, S.F. Training the Trainers in Microsurgery: A Success Story from Vietnam's Hanoi National Hospital of Odonto-stomatology. *Plastic and Reconstructive Surgery - Global Open*, 22:e3637, 2021.
8. Zhang, Y., Zhang, M., Lin, M., Gephart, M.H., Veeravagu, A., Ratliff, J., and Li, G. Costs and Complications Associated With Resection of Supratentorial Tumors With and Without the Operative Microscope in the United States. *World Neurosurgery*, 138:e607–e619, 2020.
9. Shrime, M.G., Dare, A., Alkire, B.C., and Meara, J.G. A global country-level comparison of the financial burden of surgery. *World Neurosurgery*, 103:1453–1461, 2016.
10. Ma, L., and Fei, B. Comprehensive review of surgical microscopes: technology development and medical applications. *Journal of Biomedical Optics*, 26:010901, 2021.
11. Higgins, C.G., Thomson, S.E., Baker, J., Honeyman, C., Kearns, M., Roberts, J., and Tay, S. COVID-19 lockdown and beyond: Home practice solutions for developing microsurgical skills. *Journal of Plastic, Reconstructive Aesthetic Surgery*, 74:407–447, 2021.
12. Oltean, M., Nistor, A., Hellstrom, M., Axelsson, M., Yagi, S., Kobayashi, E., Ballestin, A., Akelina, Y., and Nemeth, N. Microsurgery training during COVID-19 pandemic: Practical recommendations from the International Society for Experimental Microsurgery and International Microsurgery Simulation Society. *Microsurgery*, 41:398–400, 2021.
13. Jianmongkol, S., Vinitpairot, C., Thitiworakarn, N., and Wattanakamolchai, S. A comparison of using a smartphone versus a surgical microscope for microsurgical anastomosis in a non-living model. *Archives of Plastic Surgery*, 49:121–126, 2022.
14. Ho, D.K. Using smartphone-delivered stereoscopic vision in microsurgery: a feasibility study. *Eye (London)*, 33:953–956, 2019.
15. Koch, H., Dabernig, J., Allert, S., Puchinger, M., and Scharnagl, E. Wearable technology for global surgical teleproctoring. *Annals of Plastic Surgery*, 49(5):470–471, 2002.
16. Schindelin J., Arganda-Carreras, I., Frise, E., Kaynig, V., Longair, M., Pietzsch, T., Preibisch, S., Rueden, C., Saalfeld, S., Schmid, B., Tinevez, J., White, D.J., Hartenstein, V., Eliceiri, K., Tomancak,P., and Cardona, A. Fiji: an open-source platform for biological-image analysis. *Nature Methods*, 9(7):676–682, 2012.

Supplementary Note 1: Source Code for Webcam Address Declaration and Start/Stop

```
using System.Collections;
using System.Collections.Generic;
using TMPro;
using UnityEngine;
using UnityEngine.UI;

public class CameraScript : MonoBehaviour {
// Start is called before the first frame update
public static int currentCamIndex = 1;
WebCamTexture tex;
public RawImage display;
public TextMeshProUGUI startStopText;
int cameraRequestedWidthRes = 1920;
int cameraRequestedHeightRes = 1080;

public void SwapCamClicked() }
if (WebCamTexture.devices.Length > 0) {
currentCamIndex += 1;
currentCamIndex %= WebCamTexture.devices.Length;
if(tex != null) {
StopWebcam();
StartStopCamClicked();
} } }

public void StartStopCamClicked() {
if (tex != null) {
StopWebcam();
startStopText.text = "Start Camera";
}

else {
WebCamDevice device = WebCamTexture.devices[currentCamIndex];
tex = new WebCamTexture(device.name, cameraRequestedWidthRes, cameraRequestedHeightRes);
display.texture = tex;
tex.Play();
startStopText.text = "Stop Camera";
} }

public void StopWebcam() {
display.texture = null;
tex.Stop();
tex = null;
}

void OnEnable() {
StartStopCamClicked();
currentCamIndex += 1;
currentCamIndex %= WebCamTexture.devices.Length; } }
```